Transmission-Line Model of Noisy Electromagnetic Media

Richard R. A. Syms, *Senior Member, IEEE*, Oleksiy Sydoruk, and Laszlo Solymar

***Abstract*—A transmission-line model of thermal noise in 1-D electromagnetic (EM) media is presented that can find both the magnetic and the electric contributions to the noise in arbitrary arrangements of isotropic material. The model is used to compute the noise performance of a negative-index metamaterial slab based on split-ring resonators and rods, when magnetic and electric noise are both significant. It is shown that the former rises rapidly in the range when negative index effects are obtained, due to the lossy magnetic resonance. Results for infinite and finite media are compared, and the effect of size is discussed. Results for the slab are also compared with the indirect prediction of standard EM theory, and shown to be identical.**

***Index Terms*—Fluctuation-dissipation theorem, Johnson noise, metamaterial, negative index, thermal noise.**

I. Introduction

SINCE THE time of Johnson [1] and Nyquist [2], it has been known that dissipative electrical elements give rise to thermal noise, due to an inescapable linkage known as the fluctuation dissipation (F-D) theorem [3], [4]. In the 1950s, Rytov showed that thermal noise generates electromagnetic (EM) waves in lossy media, and that this radiation is responsible for the thermal emittance of a body. His original work was published in Russian, but accessible accounts can be found in a translation [5] and in several well-known textbooks [6]–[8]. Similar theories were also developed in the West [9], [10].

The essence of Rytov's approach was to add randomly varying source terms (often known as test sources) to the Maxwell curl equations. The properties of the sources are obtained from the F-D theorem. The sources excite noise waves (essentially Green's functions), and Rytov found the thermal radiation by summing the waves, taking into account their lack of correlation. Although very general, his method has the limitation that the Green's functions are only known analytically for a few systems. Furthermore, he carried out the summations in k-space rather than real space. While this approach allows the identification of noise propagating near a given frequency and direction, it complicates calculations for finite or inhomogeneous media. Furthermore, such calculations tend to yield significantly different results to those of infinite homogeneous media (which anyhow generate some well-known paradoxical conclusions, such as thermal noise in apparently lossless media).

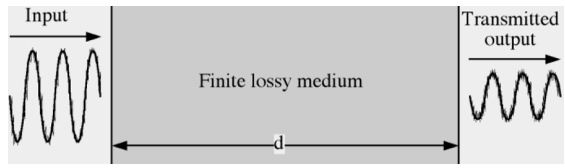

Fig. 1. EM wave incident on a slab of lossy material.

For physicists, most early interest lay in calculating the emission from extremely hot plasma [11]–[14]. Related problems include the emission of astronomical objects and radiation from nuclear detonations. Recourse was often made to approximate methods, or to an indirect method based on Kirchhoff's radiation law (for a translation of the relevant paper, see [15]), which replaces the problem of finding the emittance with that of finding the absorbance. This method again has limitations; it cannot find the noise inside a body, or separate it into electric and magnetic components.

For electrical engineers, thermal noise is of course a significant limiting factor for device performance [16]. However, while some theories of noisy circuits involve the propagation of noise waves [17]–[23], they appear to have been developed entirely in isolation from the above. The most relevant recent work on noise waves has been in photonic-bandgap structures, and considerable interest has been taken in exploiting periodicity to modify emittance [24]–[32].

By their nature, the artificial media known as metamaterials occupy an intermediate position between electrical circuits and periodically structured media. For example, although they may be described in terms of effective medium parameters, they are realized using arrangements of discrete "meta atoms," whose response is manipulated to obtain novel properties such as negative permittivity and permeability [33], [34]. Often, their behavior is modeled using equivalent circuits [35]–[40]. Since most metamaterials involve lossy conductors, the question of their thermal performance is important for a wide variety of practical applications. For example, we would expect the signal-to-noise ratio (SNR) of a wave passing through a lossy negative-index slab (Fig. 1) to deteriorate due to the additive effect of thermal noise.

We would also expect to be able to control the spectral variation of emittance to some extent, for example, to alter the radiation in a given band and hence realize novel thermal sources. However, effective methods of calculating noise are needed to assess the likely effects. In the past, the overwhelming emphasis has been on electrically generated noise. However,

Manuscript received May 18, 2012; revised October 17, 2012; accepted October 19, 2012. Date of publication December 05, 2012; date of current version January 17, 2013.

The authors are with the Electrical and Electronic Engineering Department, Imperial College London, London SW7 2AZ, U.K. (e-mail: r.syms@imperial.ac.uk; o.sydoruk@imperial.ac.uk; laszlo.solymar@hertford.ox.ac.uk).

Digital Object Identifier 10.1109/TMTT.2012.2226742

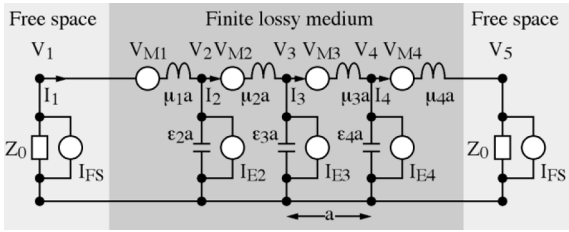

Fig. 2. Transmission-line model of a finite 1-D noisy EM slab.

because metamaterials require magnetic effects to generate simultaneously negative values of permittivity and permeability, magnetically generated noise also requires investigation.

Clearly, EM noise cannot be separated experimentally into electrically and magnetically generated components. However, knowledge of the origins of the dominant noise contribution will allow engineers to develop low-noise designs. Particularly, the poor performance of the magnetic resonators currently used in metamaterials may be identified.

Previously, we have considered the propagation of noise waves in purely magnetic metamaterials [41], [42]. Here, we demonstrate a general transmission-line model for 1-D systems, capable of performing both direct and indirect calculations, and demonstrate its use in a double negative material. The idea of modeling EM media in terms of transmission lines containing lumped-element components that describe the material properties is long established. Here we take the equivalence one step further, and use the current and voltage sources that represent the noise in the components to model the noise due to the medium. In doing so, we arrive at a discrete approximation to the Rytov model. The model is introduced in Section II. Analytic predictions for infinite media are presented in Section III and numerical calculations for finite media in Section IV. Since it is important to provide an independent verification, the numerical results are confirmed using rigorous solution of Maxwell's equations in Section V. Conclusions are drawn in Section VI.

II. 1-D Transmission-Line Model

We base the analysis on a 1-D transmission-line description of EM wave propagation. To construct the model, 1-D space is first discretized into N sections. Generally, N_{el} sections (whose equivalent circuit parameters describe local properties) will be required for the material, together with two additional sections for free space outside, so that $N = N_{el} + 2$. Fig. 2 shows an example where three central sections correspond to the medium, while the first and last represent free space. For a general slab of thickness d, $N_{el} = d/a$, where a is the period.

Within the medium, the series impedance in the nth element is a complex inductance $L_n = L'_n - \mathrm{j}L''_n = \mu_n a = (\mu'_n - \mathrm{j}\mu''_n)a$, where L'_n and L''_n are, by definition, the real and imaginary parts of the inductance and μ'_n and $\mathrm{j}\mu''_n$ are the real and imaginary parts of the complex permeability μ_n. The corresponding impedance is defined as $\mathrm{j}\omega L_n = \mathrm{j}\omega L'_n + \omega L''_n$ at angular frequency ω, where $\omega L''_n$ is a frequency-dependent series resistance. Similarly, the shunt impedance is a capacitance $C_n = \varepsilon_n a$, where $\varepsilon_n = \varepsilon'_n - \mathrm{j}\varepsilon''_n$ is the complex permittivity. Any nonzero value of ε''_n will then introduce a parallel conductance $\omega\varepsilon''_n a$. Note that both the inductance and capacitance may vary from element to element.

According to Nyquist [2], the resistances and conductances will inject thermal noise. Each series element therefore has an associated voltage source V_{Mn}, describing magnetic noise, whose root mean square (rms) value in a frequency interval $\mathrm{d}f$ is obtained from the fluctuation-dissipation theorem. At low frequency, we may use the approximation $V_{Mn}V^*_{Mn} = 4K\theta\omega\mu''_n a\ \mathrm{d}f$. Here, K is the Boltzmann's constant and θ is absolute temperature, assumed the same everywhere so the system is in thermal equilibrium. At higher frequency, the full quantum expression derived from the F-D theorem [3] may be used. Similarly, the shunt impedance has an associated current source I_{En}, describing electric noise, whose corresponding rms value is specified at low frequency by $I_{En}I^*_{En} = 4K\theta\omega\varepsilon''_n a\ \mathrm{d}f$. These sources are similarly uncorrelated, and there is no correlation between magnetic and electric noise. In general, the correlation properties of the sources may therefore be summarized as [5]

$$\begin{aligned} V_{Mn}V^*_{Mm} &= 4K\theta\omega\mu''_n a\ \mathrm{d}f\ \delta_{nm} \\ I_{En}I^*_{Em} &= 4K\theta\omega\varepsilon''_n a\ \mathrm{d}f\ \delta_{nm} \\ V_{Mn}I^*_{Em} &= 0. \end{aligned} \tag{1}$$

Here, * denotes the complex conjugate and δ_{nm} is the Kronecker delta. The general task is to find the system response with all sources present. Within the medium, the transmission-line equations are

$$\begin{aligned} V_{n+1} - V_n &= -\mathrm{j}\omega\mu_n a I_n + V_{Mn} \\ I_n - I_{n-1} &= -\mathrm{j}\omega\varepsilon_n a V_n + I_{En}. \end{aligned} \tag{2}$$

These equations are clearly analogous to the time-independent Maxwell curl equations, with V_n and I_n representing the electric and magnetic fields, respectively, and V_{Mn} and I_{En} representing Rytov's sources. For slow variations, we would therefore expect the quantity $Z_n = \sqrt{(\mu_n/\varepsilon_n)}$ to describe the local impedance. If we then write $\mu_n = \mu_0\mu_{rn}$ and $\varepsilon_n = \varepsilon_0\varepsilon_{rn}$, where the subscripts 0 and r indicate free space and relative quantities, respectively, we would also expect the quantity $\sqrt{(\mu_{rn}\varepsilon_{rn})}$ to describe the local refractive index.

The line is terminated at each end with a real impedance $Z_0 = \sqrt{(\mu_0/\varepsilon_0)}$, to represent free space. For these elements, the equations are different, and given by

$$\begin{aligned} I_1 &= \frac{-V_1}{Z_0} + I_{\mathrm{FS}} \\ -I_{N-1} &= \frac{-V_N}{Z_0} + I_{\mathrm{FS}}. \end{aligned} \tag{3}$$

Here, terms I_{FS} are noise sources associated with free space, whose rms value is specified by $I_{\mathrm{FS}}I^*_{\mathrm{FS}} = (4K\theta/Z_0)\ \mathrm{d}f$.

The equations can be written in matrix form as $\underline{M}\ \underline{Y} = \underline{X}$. Here, $\underline{M}$ is an $N_M \times N_M$ matrix, $\underline{Y}$ is a N_M-element column vector containing the nodal voltages and line currents, $\underline{X}$ is a N_M-element column vector containing the noise voltages and currents, and $N_M = 2N - 1$. Equation (4) shows the corresponding matrix representation. The matrix $\underline{M}$ is clearly tridi-

agonal, and its diagonal elements consist of local admittances, shown in (4), at the bottom of this page.

The unknowns can be found for any input as $\underline{Y} = \underline{M}^{-1}\underline{X}$. Solution of N_M simultaneous equations in this way clearly involves inversion of an $N_M \times N_M$ matrix, which becomes increasingly time consuming as N_M rises. However, some problems—for example, those involving slabs—may contain uniform sections of significant length. Within these regions, the noise wave solutions can only take the form of standing waves, whose description requires only two current wave amplitude coefficients. If these regions may be identified, it should be possible to reduce the number of equations that must be solved, effectively trading a reduction in execution time for an increase in algorithm complexity.

Since the sources are not correlated, the local noise due to the material may be found directly by evaluating $\underline{Y}$ for each source in the line in turn and performing an incoherent addition of the results. This process is equivalent to the spatial summation of a set of numerically calculated Green's functions, which are unique to the arrangement considered. For example, if the current in element n due to a magnetic noise source V_{Mm} in element m is I_{Mnm} and the corresponding current due to an electric noise source I_{Em} in element m is I_{Enm}, the local noise power is $P_n = P_{Mn} + P_{En}$, where

$$P_{Mn} = \sum_m I_{Mnm} I^*_{Mnm} Re(Z_n)$$
$$P_{En} = \sum_m I_{Enm} I^*_{Enm} \mathrm{Re}(Z_n). \tag{5}$$

Here, the summations are taken over all source positions m.

The powers P_{Mn}, P_{En}, and P_n can be written in terms of spectral densities p_{Mn}, p_{En}, and p_n, such that $p_{Mn} = P_{Mn}/\mathrm{d}f$, and so on. Calculation of the spectral density p_N in, say, the right-hand load, then allows direct calculation of the emittance E (the ratio of the thermal power emitted to the power emitted by a black body at the same temperature θ) as

$$E = \frac{p_N}{K\theta}. \tag{6}$$

This quantity may also be subdivided into magnetically and electrically driven contributions E_M and E_E. Other quantities may be found by evaluating $\underline{Y}$ when the noise arises instead from, say, the left-hand free-space impedance. In this case, the reflection coefficient and transmission coefficients are

$$r = \frac{\left(\frac{V_1}{I_1} - Z_0\right)}{\left(\frac{V_1}{I_1} + Z_0\right)}$$
$$t = \frac{(1+r)V_N}{V_1}. \tag{7}$$

The reflectance and transmittance are then $R = |r|^2$ and $T = |t|^2$, respectively. Assuming that the input signal power is P_S, and the input source noise power in a bandwidth $\mathrm{d}f$ is $P_{\mathrm{SN}} = K\theta \mathrm{d}f$, the input SNR is P_S/P_{SN}. After passing through the slab, both P_S and P_{SN} will be modified by the transmittance T. However, P_{SN} will also be augmented by the noise due to the medium $P_N = EK\theta\ \mathrm{d}f$. Thus, the output signal power is ${P_S}' = P_S T$, while the output noise power is ${P_{\mathrm{SN}}}' = P_{\mathrm{SN}}T + P_N$. The output SNR is therefore ${P_S}'/{P_{\mathrm{SN}}}'$, and the noise factor F—the input SNR divided by the output SNR—can be obtained as

$$F = 1 + \frac{E}{T}. \tag{8}$$

The noise figure (NF) is then $\mathrm{NF} = 10\log_{10}(F)$.

By comparison, the indirect method uses Kirchhoff's law of thermodynamic equilibrium to argue for the equivalence between the emittance and the absorbance A, leading to the alternative expression for the noise factor

$$F = 1 + \frac{A}{T}. \tag{9}$$

The absorbance can of course be found from the transmittance and reflectance as $A = 1 - R - T$. This approach allows the noise properties of a body to be found by probing it externally. However, it clearly cannot separate the emittance into magnetically and electrically generated parts.

III. Infinite Homogeneous Media

Before proceeding to specific examples, we consider the case of infinite homogeneous media, for which we can ignore the terminations and write $\mu_n = \mu$ and $\varepsilon_n = \varepsilon$ for all n in (1) and (2). The problem can then be solved in terms of known Green's functions.

$$\begin{bmatrix} \frac{1}{Z_0} & 1 & 0 & 0 & 0 & 0 & 0 \\ -1 & \mathrm{j}\omega\mu_1 a & 1 & 0 & 0 & 0 & 0 \\ 0 & -1 & \mathrm{j}\omega\varepsilon_2 a & 1 & 0 & 0 & 0 \\ 0 & 0 & -1 & \mathrm{j}\omega\mu_2 a & 0 & 0 & 0 \\ & & & & & & \\ 0 & 0 & 0 & 0 & \mathrm{j}\omega\varepsilon_{N-1} a & 1 & 0 \\ 0 & 0 & 0 & 0 & -1 & \mathrm{j}\omega\mu_{N-1} a & 1 \\ 0 & 0 & 0 & 0 & 0 & -1 & \frac{1}{Z_0} \end{bmatrix} \begin{bmatrix} V_1 \\ I_1 \\ V_2 \\ I_2 \\ \\ V_{N-1} \\ I_{N-1} \\ V_N \end{bmatrix} = \begin{bmatrix} I_{\mathrm{FS}} \\ V_{M1} \\ I_{E2} \\ V_{M2} \\ \\ I_{EN-1} \\ V_{MN-1} \\ I_{\mathrm{FS}} \end{bmatrix} \tag{4}$$

We first note that, in the absence of sources, (2) may be uncoupled. Assumption of the traveling-wave solutions $I_n = I_0 \exp(-jnka)$ or $V_n = V_0 \exp(-jnka)$, where $k = k' - \mathrm{j}k''$ is the complex propagation constant, then yields the standard dispersion relation

$$\omega^2 \mu\varepsilon a^2 - 2\{1 - \cos(ka)\} = 0. \tag{10}$$

When ka is small (generally the case), we obtain the standard result $k^2 = \omega^2\mu\varepsilon$. If we then write $\mu = \mu_0\mu_r$ and $\varepsilon = \varepsilon_0\varepsilon_r$, this approximation leads directly to the interpretation of $\sqrt{(\mu_r\varepsilon_r)}$ as the refractive index n, as assumed before. However, since it may be complex, we write $n = n' - \mathrm{j}n''$ and choose the sign of the square root to give decaying rather than growing waves. Similarly, the characteristic impedance is the constant $Z = \sqrt{(\mu/\varepsilon)}$ where the sign of the square root is chosen to give a positive real part.

We now consider the effect of the source terms. Initially, we consider the magnetic noise excited by the presence of single voltage source V_{M0} in element 0, as shown in Fig. 3(a).

For this case, (2) may be solved by assuming that the source excites a symmetric pattern of current waves propagating away in either direction, namely,

$$I_{Mn} = I_{M0} \exp(-\mathrm{j}|n|ka). \tag{11}$$

This solution is the Green's function for magnetically excited noise waves in an infinite homogeneous medium, written in terms of currents. Substitution of (11) into (2), and making use of (10) allows the amplitude I_{M0} to be found. Using the approximation of small ka once again, we obtain $I_{M0} = (V_{M0}/2)\sqrt{(\varepsilon/\mu)}$. Since we may write this result as $I_{M0} = V_{M0}/2Z$, it has a simple interpretation: it is the current we would expect to launch into two semi-infinite 1-D media arranged in parallel. Accompanying the current waves are voltage waves. At the same level of approximation, it is simple to show that their pattern is antisymmetric and given by

$$\begin{aligned} V_{Mn} &= -\left(\frac{I_{M0}k}{\omega\varepsilon}\right)\exp(+jnka), \qquad \text{for } n \le 0 \\ V_{Mn} &= +\left(\frac{I_{M0}k}{\omega\varepsilon}\right)\exp[-\mathrm{j}(n-1)ka], \qquad \text{for } n \ge 1. \end{aligned} \tag{12}$$

Since the sources are uncorrelated, the Green's functions must be so as well. To allow their incoherent addition, we will generally be interested terms of the form $I_{Mn}I^*_{Mn}$, which, in this case, may clearly be written as

$$I_{Mn}I^*_{Mn} = I_{M0}I^*_{M0} \exp(-2|n|k''a). \tag{13}$$

Since the noise sources are all identical, the current I_{Mnm} in element n due to a source in a different element m can then be written down straightaway as the shifted solution

$$I_{Mnm}I^*_{Mnm} = I_{M0}I^*_{M0} \exp(-2|n-m|k''a). \tag{14}$$

Fig. 3(b) shows example variations for representative noise sources. The patterns decay exponentially on either side of the excitation. At each point, their effects must be summed,

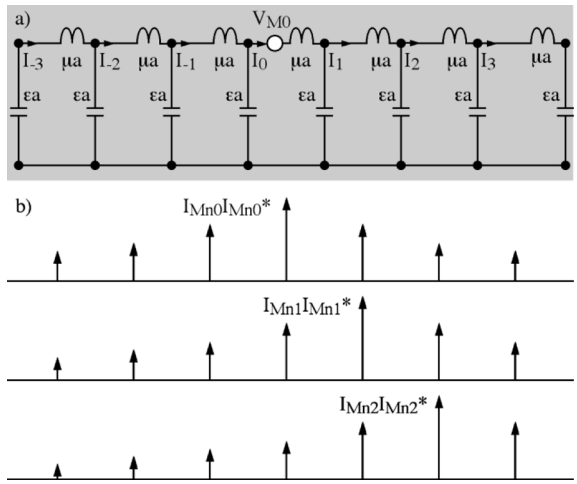

Fig. 3. (a) Infinite homogeneous medium with magnetic noise source in element 0. (b) Current distributions from representative noise sources.

but for infinite homogeneous media, the result must be independent of position. We therefore need only consider one observation point, say, element 0. Since the current I_{M0m} in this element due to a source in element m must satisfy $I_{M0m}I^*_{M0m} = I_{M0}I^*_{M0}\exp(-2|m|k''a)$, the total effect due to all the magnetic noise sources is the incoherent sum

$$I_M I^*_M = I_{M0}I^*_{M0} \sum_{m=-\infty}^{\infty} \exp(-2|m|k''a). \tag{15}$$

Assuming $k''a$ is small, this sum can be evaluated analytically, to get $I_M I^*_M = I_{M0}I^*_{M0}/k''a$. The corresponding power (the same everywhere) is then $P_M = I_M I^*_M \mathrm{Re}(Z)$. With some simple manipulation, we then obtain for the spectral density of magnetically excited noise

$$p_M = K\theta\sqrt{\left(\frac{\varepsilon_r\varepsilon_r^*}{\mu_r\mu_r^*}\right)}\,\mathrm{Re}\left\{\sqrt{\left(\frac{\mu_r}{\varepsilon_r}\right)}\right\}\frac{\mu_r''}{n''}. \tag{16}$$

The analysis above may be repeated for electric noise, starting by assuming a current source I_{E0} in element 0. The main steps are similar; however, this time the Green's function $V_{Mn} = V_{M0}\exp(-\mathrm{j}|n|ka)$ for voltage waves is symmetric, and the associated current pattern is antisymmetric. The resulting spectral density of electrically excited noise is

$$p_E = K\theta\sqrt{\left(\frac{\mu_r\mu_r^*}{\varepsilon_r\varepsilon_r^*}\right)}\,\mathrm{Re}\left\{\sqrt{\left(\frac{\varepsilon_r}{\mu_r}\right)}\right\}\frac{\varepsilon_r''}{n''}. \tag{17}$$

Equations (16) and (17) clearly have similar form, and can be obtained from each other by exchanging magnetic and electric quantities. Since the two types of noise are also uncorrelated, the total spectral density can again be written as $p = p_M + p_E$.

We now briefly consider the paradox of noise in low-loss media. If $\varepsilon_r'' \ll \varepsilon_r'$ and $\mu_r'' \ll \mu_r'$, we can make the approximations $\sqrt{(\varepsilon_r\varepsilon_r^*/\mu_r\mu_r^*)} \approx \varepsilon_r'/\mu_r'$, $\mathrm{Re}\{\sqrt{(\mu_r/\varepsilon_r)}\} \approx \sqrt{(\mu_r'/\varepsilon_r')}$, $n' \approx \sqrt{(\mu_r'\varepsilon_r')}$, and

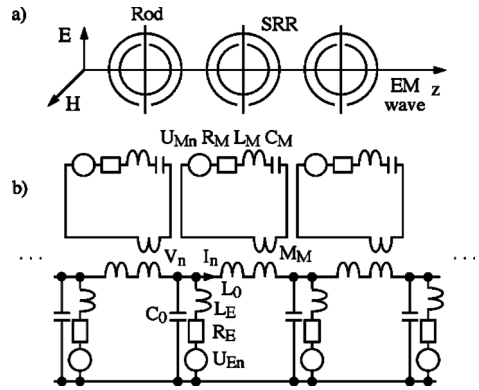

Fig. 4. Negative index medium based on SRRs and rods. (a) Physical realization. (b) Circuit representation.

$n'' = \{\mu_r'\varepsilon_r'' + \varepsilon_r'\mu_r''\}/\{2\sqrt{(\mu_r'\varepsilon_r')}\}$. In this case, we obtain

$$p_M \approx \frac{2K\theta\ \varepsilon_r'\mu_r''}{\{\mu_r'\varepsilon_r'' + \varepsilon_r\mu_r''\}}$$
$$p_E \approx \frac{2K\theta\ \mu_r'\varepsilon_r''}{\{\mu_r'\varepsilon_r'' + \varepsilon_r'\mu_r''\}}. \tag{18}$$

Addition then leads to the result $p = 2K\theta$, corresponding to $K\theta$ for each of the two wave directions. This result still holds when losses tend to 0, and implies that there must actually be thermal noise in lossless media, a well-known and counter-intuitive conclusion. However, the paradox is resolved by considering that the noise must be generated by a summation of an infinite set of infinitely weak noise waves with contributions arising from sources infinitely far from the point of observation. Consequently, similar effects cannot arise in more realistic finite media.

IV. Noise in Negative Index Media

As an example, we consider the case of noise in negative index media, a topic of current interest. In such media, magnetic resonators such as split-ring resonators (SRRs) are used to control the effective relative magnetic permeability μ_r at RF and microwave frequencies [33], [34]. Similarly, conducting rods are used to control the dielectric permittivity ε_r. With careful choice of parameters, μ_r and ε_r may each be made negative over limited frequency ranges. In any range where both are simultaneously negative, the refractive index $n = \sqrt{(\varepsilon_r\mu_r)}$ is also negative, and many interesting phenomena such as negative refraction can arise.

SRRs consist of a nested pair of conducting loops with splits located on opposite sides. In the 1-D case, the SRRs are arranged perpendicular to the magnetic field of a traveling EM wave, as shown in Fig. 4(a). In this geometry, the magnetic field can induce voltages in the resonators. The resulting currents create additional magnetic fields, which, when added to the original field, give rise to the effect of nonunity relative permeability. Similarly, the rods are conducting strips. These are arranged parallel to the electric field, which may then drive currents up and down the strips. The currents then give rise to additional electric fields, which are in turn responsible for the effect of nonunity relative permittivity. Thus, magnetic and dielectric effects may both be achieved using conductors. However, the presence of loss in the conductors makes such media particularly susceptible to noise.

Assuming that the SRRs are not coupled to their neighbors, a detailed equivalent circuit valid for low frequency is as shown in Fig. 4(b) [39]. Here, the EM wave is represented as a transmission line with lossless series and parallel elements $L_0 = \mu_0 a$ and $C_0 = \varepsilon_0 a$. SRR loading is represented using lossy L–C resonators with elements R_M, L_M, and C_M, coupled via a mutual inductance M_M into the series branch. Rod loading is represented using inductances L_E and resistances R_E in the shunt branch. Associated with R_M and R_E are noise sources U_{Mn} and U_{En}. Their values follow from the F-D theorem, and satisfy $U_{Mn}U_{Mn}^* = 4K\theta R_M\ \mathrm{d}f$ and $U_{En}U_{En}^* = 4K\theta R_E\ \mathrm{d}f$ [2].

In this equivalent circuit, all the components and noise sources have constant values, but the circuit is relatively complex. However, it is straightforward to reduce it to the simpler form shown in Fig. 2, where the permittivity and permeability are now frequency dependent and given by

$$\varepsilon_r = 1 - \frac{\omega_p^2}{(\omega^2 - \mathrm{j}\omega\omega_\tau)}$$
$$\mu_r = 1 - \frac{q^2}{\left(1 - \frac{\omega_0^2}{\omega^2} - \frac{\mathrm{j}\omega_0}{\omega Q_0}\right)}. \tag{19}$$

Here, $\omega_0 = 1/\sqrt{(L_M C_M)}$ is the resonant frequency of the resonators, $Q_0 = \omega_0 L_M/R_M$ is their quality factor, $q^2 = M_M^2/L_0 L_M$ is the filling factor, and $\omega_p = 1/\sqrt{(L_E C_0)}$ and $\omega_\tau = R_E/L_E$ are the equivalent plasma frequency and collision damping frequency of the rods, respectively. Similarly, it is possible to show that the noise sources are related to the imaginary parts of the permittivity and permeability, as previously described.

Fig. 5 shows the frequency dependence of the effective medium parameters for $a = 1$ cm, $\omega_0 = c/10a$, where $c = 1/\sqrt{(\mu_0\varepsilon_0)}$, corresponding to a resonant frequency of 480 MHz, $Q_0 = 200$, $q^2 = 0.1$, $\omega_p/\omega_0 = 1.1$, and $\omega_\tau/\omega_0 = 0.01$. Here, we focus on the frequency range for which negative parameters are obtained.

The real part of ε_r [see Fig. 5(a)] is slowly varying, being negative below the plasma frequency ω_P and positive above it, and tending to unity at high frequency. The real part of μ_r [see Fig. 5(b)] is much faster varying, being positive below the resonant frequency ω_0, negative just above it and again tending to unity at high frequency. The real part of the index [see Fig. 5(c)] has a more complicated variation. n' is approximately 0 when ε_r' and μ_r' are of opposite signs. When both are negative, n' is negative, and when both are positive, n' has a conventional positive value. The imaginary part of the permittivity ε_r'' is generally small and slowly varying. However, because the magnetic effects are derived from a resonance, μ_r'' has a large peak near ω_0. Consequently, we would expect n'' to be dominated by magnetic loss, and hence, that propagation loss would be high in exactly the region where negative-index effects are obtained. In this range, we would therefore expect poor noise performance.

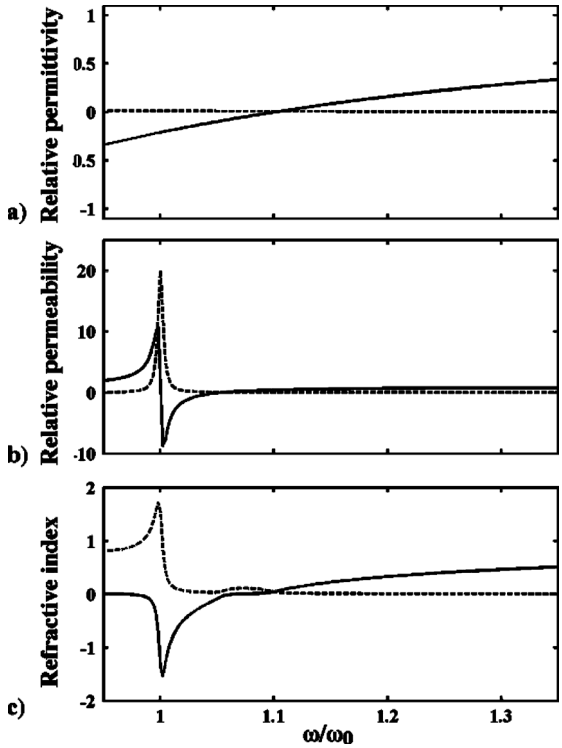

Fig. 5. Frequency variations of: (a) ε_r, (b) μ_r, and (c) n for a negative index medium. Solid lines: real part. Dashed lines: imaginary part.

Fig. 6 shows the frequency variations of the normalized magnetic, electric, and total noise power spectral densities $p_M/2K\theta$, $p_E/2K\theta$, and $p/2K\theta$ for an infinite medium under different conditions. The parameters are generally as above.

However, in Fig. 6(a), we arbitrarily set ω_p and ω_τ to 0 to mimic the effect of removing the rods. There is only magnetic noise, and $p_M \approx 2K\theta$ in the passbands where $\mu_r' > 0$, and $p_M \approx 0$ in the stopband where $\mu_r' < 0$. Similarly, in Fig. 6(b), we restore the rods, but set q^2 to 0 to mimic the effect of removing the resonators. There is now only electric noise, and $p_E \approx 2K\theta$ when $\varepsilon_r' > 0$, and $p_E \approx 0$ when $\varepsilon_r' < 0$. In Fig. 6(c), we allow rods and resonators together so both types of noise are present. This time, the total noise density is $p \approx 2K\theta$ in the propagating bands, when μ_r' and ε_r' have the same sign, but $p \approx 0$ when the signs differ. For these parameters, magnetic noise dominates in the negative index band.

To highlight the difference between finite and infinite media, Fig. 7 shows the frequency variations of $p_M/2K\theta$, $p_E/2K\theta$, and $p/2K\theta$ at the center of the slab, when resonators and rods are both present.Fig. 7(a)–(c) shows results for $N_{el} = 100, 500,$ and 2500, respectively (corresponding to $d = 1, 5,$ and 25 m). For small N_{el}, the spectra are very different to those of Fig. 6(c), and the noise is generally lower in the low-loss spectral region above ω_p. As N_{el} rises, the results gradually approach those for infinite media, but become increasingly oscillatory. These effects arise from a combination of the absence of some of the long-range noise sources that contribute to the uniform noise density in an infinite medium, and Fabry–Perot effects in the slab. Note that the convergence is extremely slow, highlighting the unrealistic nature of the results for infinite media.

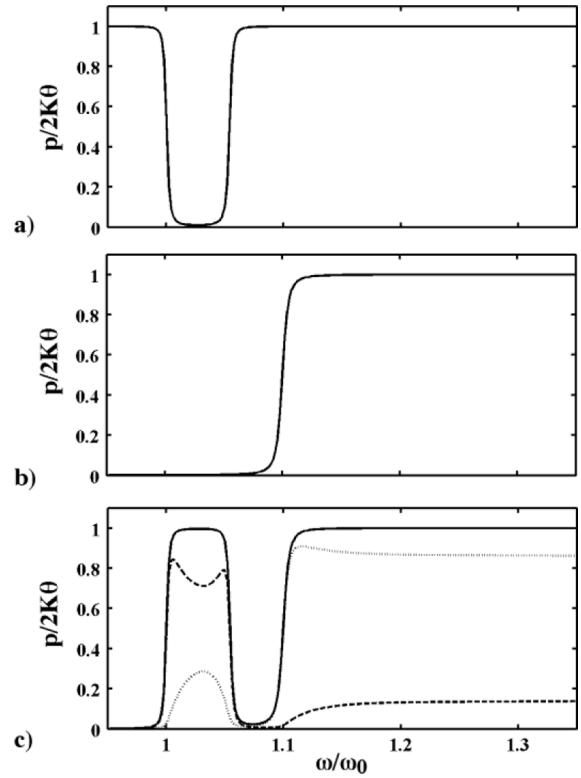

Fig. 6. Frequency variation of the normalized noise PSD $p/2K\theta$ in an infinite medium based on: (a) resonators only, (b) rods only, and (c) resonators and rods together. Dashed lines: magnetic noise. Dotted: electric noise. Solid: total.

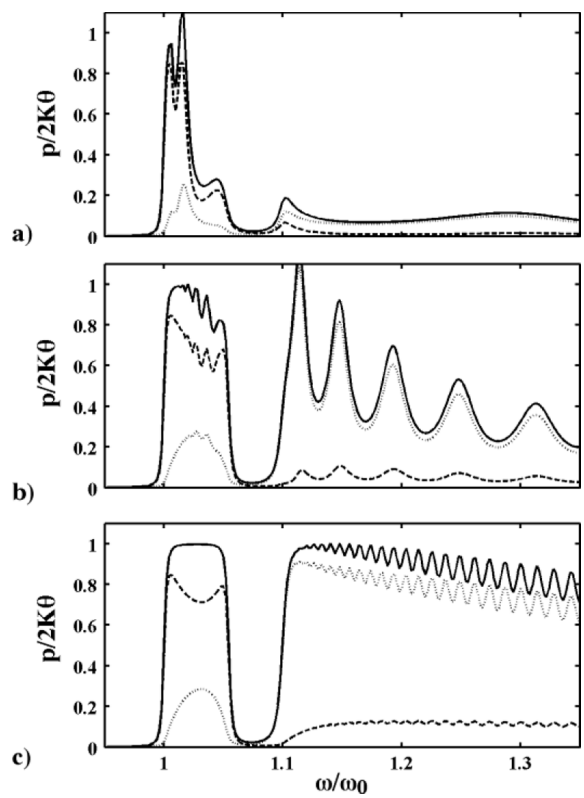

Fig. 7. Frequency variation of the normalized noise PSD $p/2K\theta$ at the center of a finite slab based on resonators and rods for: (a) 100, (b) 500, and (c) 2500 elements. Dashed lines: magnetic noise. Dotted: electric noise. Solid: total.

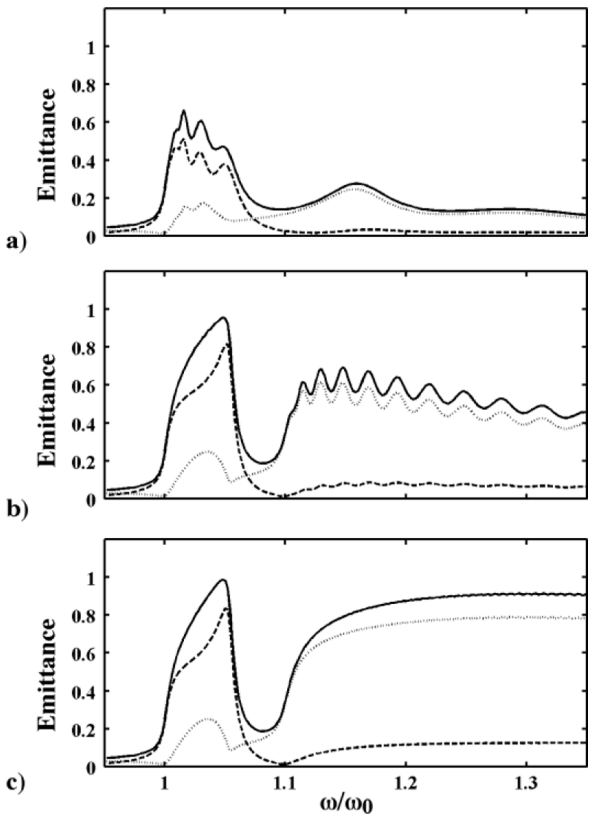

Fig. 8. Frequency variation of the emittance E of a finite slab based on resonators and rods for: (a) 100, (b) 500, and (c) 2500 elements. Dashed lines: magnetic noise. Dotted: electric noise. Solid: total.

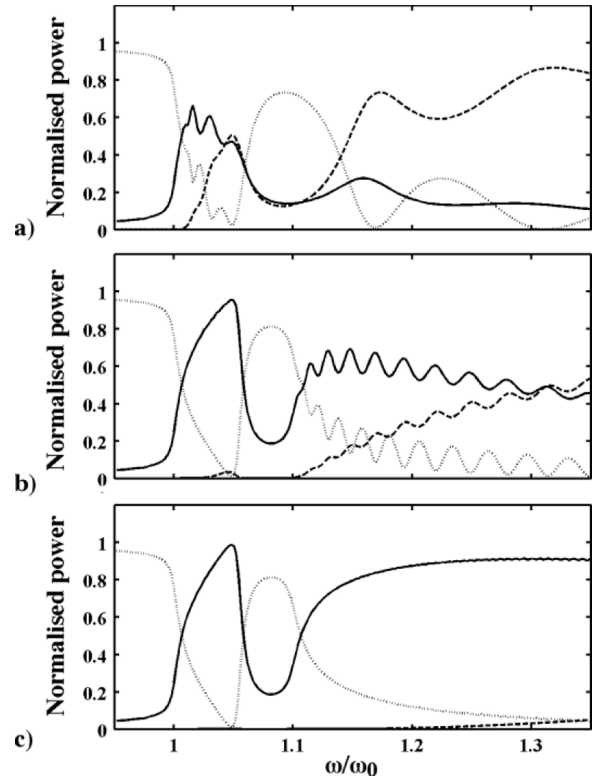

Fig. 9. Frequency variation of the transmittance T (dashed lines), reflectance R (dotted), and emittance E (solid) of a finite slab based on resonators and rods for: (a) 100, (b) 500, and (c) 2500 elements.

Fig. 8 shows the corresponding data for the emittance. Once again, the results gradually evolve as N_{el} rises so that the emittances of thick and thin slabs are quantitatively different. However, once the slab is thick enough, the emittance becomes effectively constant and the slab may be considered infinite for all practical purposes.

Fig. 9 shows the corresponding variations of the transmittance, reflectance, and emittance, all plotted together. Again, we see differences as the slab thickness changes. However, once the slab is thick enough, its reflectance also effectively becomes constant, while its transmittance tends to 0.

The behavior above implies poor noise performance for thick slabs. Fig. 10 shows the corresponding frequency variation of the NF. For small thickness, the NF rises rapidly as n' becomes increasingly negative, reaching a peak at ω_0. Since the frequency range in which n' is negative approaches this value, the operating frequencies of negative index media based on magnetic resonators should be chosen with care. As the thickness rises, usable NFs are obtained only at high frequency, i.e., completely outside the negative index band. As has previously been noted [41], [42], amplification may be used to restore the signal, but will be unable to improve the NF significantly. High-Q-factor SRRs are therefore imperative.

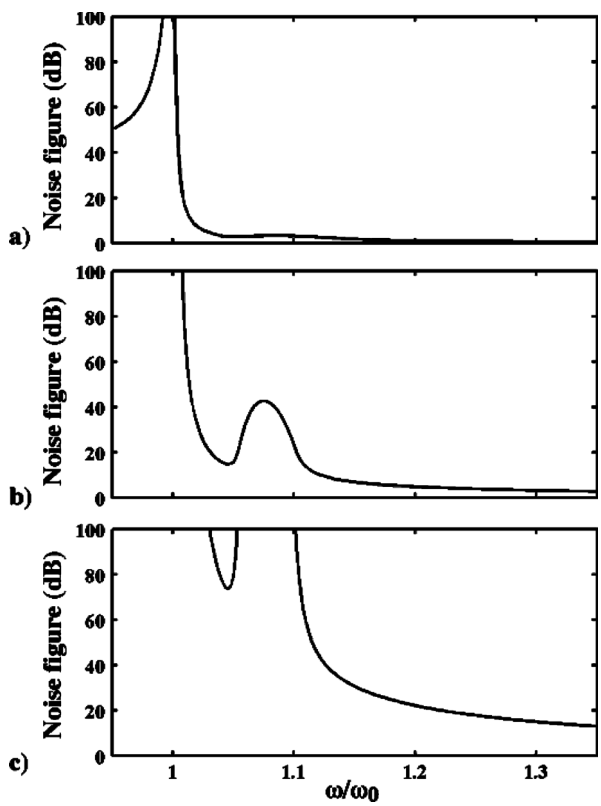

Fig. 10. Frequency variation of the NF of a finite slab based on resonators and rods for: (a) 100, (b) 500, and (c) 2500 elements.

V. Verification Using Maxwell's Equations

For some simple arrangements, the results may be compared with the prediction of standard EM theory. All that is required is a method of finding the transmittance and the reflectance. If one is available, the absorbance can be extracted and Kirchhoff's

law invoked to find the emittance. For example, for a uniform slab, the transmission and reflection coefficients are

$$t = \frac{t_{12}t_{21}\exp(-jk_0nd)}{\{1 - r_{21}^2\exp(-\mathrm{j}2k_0nd)\}}$$
$$r = r_{12} + \frac{t_{12}t_{21}r_{21}\exp(-\mathrm{j}2k_0nd)}{\{1 - r_{21}^2\exp(-\mathrm{j}2k_0nd)\}}. \quad (20)$$

Here, $k_0 = \omega/\sqrt{(\varepsilon_0\mu_0)}$ is the propagation constant of free space and r_{ij} and t_{ij} are the transmission and reflection coefficients at the interface between media i and j given by

$$r_{12} = \frac{\left(1 - \frac{n}{\mu_r}\right)}{\left(1 + \frac{n}{\mu_r}\right)} = -r_{21}$$
$$t_{12} = \frac{2}{\left(1 + \frac{n}{\mu_r}\right)} \quad t_{21} = \frac{2(\frac{n}{\mu_r})}{(1 + (\frac{n}{\mu_r}))}. \quad (21)$$

The transmittance and reflectance may then be found as $R = |r|^2$ and $T = |t|^2$. Using this approach, exactly the same results as Figs. 9 and 10 were obtained, confirming the essential validity of the transmission-line model. However, the indirect method clearly cannot make any predictions for infinite media, find the noise inside a body, separate the magnetic and electric contributions, or perform calculations for general geometries.

Some differences were seen when the same slab thickness was modeled using smaller numbers of elements with larger values of the period a. These departures are due to increasing granularity in the numerical model, which then provides a less effective representation of a continuous medium. Clearly, an appropriate subdivision of the calculation space is required to achieve accurate results.

VI. Conclusions

We have demonstrated a simple 1-D transmission-line calculator for EM noise. The method allows both the magnetic and electric contributions to the emittance and noise factor to be found, together with transmittance and reflectance, and should therefore be useful in general noise calculations. The significant difference between the "classical" result for the power spectral density of noise in infinite media and the more realistic result obtained in finite slabs has been highlighted.

The model is clearly based on low-frequency assumptions and has restricted dimension. The use of a circuit analog is no disadvantage since it should simplify the addition of sources and detectors, and hence, allow the simulation of complete communication or sensing systems. A 1-D model should be adequate for many problems involving slabs, shells, and multilayers, and extension of the method to describe other media and include additional dimensions appears possible.

For example, simulation of signal propagation in 2-D and 3-D metamaterials has already been carried out [37], [38]. The development of analogous methods for modeling the propagation of noise in higher dimensions would, in principle, be straightforward. However, there are a number of practical difficulties. The first is to achieve sufficiently rapid calculation. For example, a 2-D calculation window with $N \times N$ elements would require inversion of an $N_M^2 \times N_M^2$ matrix, and computation of the effects of $2N_M^2$ noise sources. This poor size scaling might render the approach impractical for three dimensions. The second is to define absorbing boundary elements that operate effectively over a wide range of incidence angles. The third is to decompose the resulting radiation field into an angular spectrum of plane waves. These aspects are currently being considered.

The particular case of negative index media based on SRRs and rods, when magnetic effects are significant, has been examined. The results show that the NF increases rapidly in the range where the index is negative, due primarily to magnetic noise from lossy resonators used to generate a negative permeability. This conclusion represents a characteristic difference between conventional and artificial materials. Although resonance also occurs in conventional media, due to electronic or molecular absorption, high performance may easily be obtained because the quality factor is typically much higher and the operating frequency may be well separated from the resonance.

Experimental confirmation of the theoretical predictions could be carried out in a rectangular waveguide, by comparing the power spectral density of the noise due to a source such a noise diode, with and without loading by SRRs and rods between the source and receiver. However, high frequencies would be required to achieve a compact waveguide arrangement.

References

[1] J. B. Johnson, "Thermal agitation of electricity in conductors," *Phys. Rev.*, vol. 32, no. 1, pp. 87–109, Jul. 1928.

[2] H. Nyquist, "Thermal agitation of electric charge in conductors," *Phys. Rev.*, vol. 32, no. 1, pp. 110–113, Jul. 1928.

[3] H. B. Callen and T. A. Welton, "Irreversibility and generalized noise," *Phys. Rev.*, vol. 83, no. 1, pp. 34–40, Jul. 1951.

[4] R. Kubo, "The fluctuation dissipation theorem," *Rep. Prog. Phys.*, vol. 29, no. 1, pp. 255–284, Jan. 1966.

[5] S. M. Rytov, "Theory of electrical fluctuations and thermal radiation," Transl.: as AFCRC-TR-59-162 Acad. Sci., Moscow, Russia, 1953.

[6] L. D. Landau and E. M. Lifshitz, *Electrodynamics of Continuous Media*. Oxford, U.K.: Pergamon, 1960.

[7] Sh. Kogan, *Electronic Noise and Fluctuations in Solids*. Cambridge, U.K.: Cambridge Univ. Press, 1996.

[8] H. L. Pecseli, *Fluctuations in Physical Systems*. Cambridge, U.K.: Cambridge Univ. Press, 2000.

[9] H. A. Haus, "Thermal noise in dissipative media," *J. Appl. Phys.*, vol. 32, no. 3, pp. 493–500, Mar. 1961.

[10] M. Vanwormhoudt and H. A. Haus, "Thermal noise in lossy electromagnetic media," *J. Appl. Phys.*, vol. 32, no. 8, pp. 2577–2752, Aug. 1962.

[11] J. M. Boyd, "Emission of radio noise by plasmas," *Phys. Fluids*, vol. 7, no. 1, pp. 59–63, Jan. 1964.

[12] R. P. Mercier, "The radio-frequency emission coefficient of a hot plasma," *Proc. Phys. Soc.*, vol. 83, no. 5, pp. 819–822, May 1964.

[13] T. Birmingham, J. Dawson, and C. Oberman, "Radiation processes in plasmas," *Phys. Fluids*, vol. 8, no. 2, pp. 297–307, Feb. 1965.

[14] G. Bekefi, *Radiation Processes in Plasmas*. New York: Wiley, 1996.

[15] G. Kirchhoff, "On the relation between the radiating and absorbing powers of different bodies for light and heat," *Phil. Mag.*, ser. 4, vol. 20, pp. 1–21, 1860.

[16] H. T. Friis, "Noise figure of radio receivers," *Proc. IRE*, vol. 32, no. 7, pp. 419–422, Jul. 1944.

[17] H. Rothe and W. Dahlke, "Theory of noisy fourpoles," *Proc. IRE*, vol. 44, no. 6, pp. 811–818, Jun. 1956.

[18] P. Penfield, "Wave representation of amplifier noise," *IRE Trans. Circuit Theory*, vol. CT-9, no. 1, pp. 83–84, Mar. 1962.

[19] H. Bosma, "On the theory of linear noisy systems," Ph.D. dissertation, Dept. Elect. Eng., Tech. Hogeschool Eindhoven, Eindhoven, The Netherlands, 1967.

[20] R. P. Meys, "A wave approach to the noise properties of linear microwave devices," *IEEE Trans. Microw. Theory Techn.*, vol. MTT-26, no. 1, pp. 34–37, Jan. 1978.
[21] H. P. Hecken, "Analysis of linear noisy two-ports using scattering waves," *IEEE Trans. Microw. Theory Techn.*, vol. MTT-29, no. 10, pp. 997–1004, Oct. 1981.
[22] N. G. Kanaglekar, R. E. McIntosh, and W. E. Bryant, "Wave analysis of noise in interconnected multiport networks," *IEEE Trans. Microw. Theory Techn.*, vol. MTT-35, no. 2, pp. 112–116, Feb. 1987.
[23] S. Withington, "Scattered noise waves in microwave and mm-wave networks," *Microw. J.*, vol. 32, no. 6, pp. 169–178, Jun. 1989.
[24] E. Yablonovitch, "Inhibited spontaneous emission in solid-state physics and electronics," *Phys. Rev. Lett.*, vol. 58, no. 20, pp. 2059–2062, May 1987.
[25] C. M. Cornelius and J. P. Dowling, "Modification of Planck blackbody radiation by photonic bandgap structures," *Phys. Rev. A, Gen. Phys.*, vol. 59, no. 6, pp. 4736–4746, Jun. 1999.
[26] S.-Y. Lin, J. G. Fleming, E. Chow, J. Bur, K. K. Choi, and A. Goldberg, "Enhancement and suppression of thermal emission by a three-dimensional photonic crystal," *Phys. Rev. B, Condens. Matter*, vol. 62, no. 4, pp. R2243–R2246, Jul. 2000.
[27] Z. Y. Li, "Modified thermal radiation in three-dimensional photonic crystals," *Phys. Rev. B, Condens. Matter*, vol. 66, no. 24, pp. 241103–241106, Dec. 2002.
[28] S.-Y. Lin, J. G. Fleming, and I. El-Kady, "Three-dimensional photonic-crystal emission through thermal excitation," *Opt. Lett.*, vol. 28, no. 20, pp. 1909–1911, Oct. 2003.
[29] C. Luo, A. Narayanaswamy, G. G. Chen, and J. D. Joannopoulos, "Thermal radiation from photonic crystals: A direct calculation," *Phys. Rev. Lett.*, vol. 93, no. 93, p. 213905, Nov. 2004.
[30] I. El-Kady, W. W. Chow, and J. G. Fleming, "Emission from an active photonic crystal," *Phys. Rev. B, Condens. Matter*, vol. 72, no. 19, p. 195110, Nov. 2005.
[31] D. L. C. Chan, M. Soljacic, and J. D. Joannopoulos, "Direct calculation of thermal emission for three-dimensionally periodic photonic crystal slabs," *Phys. Rev. E, Stat. Phys. Plasmas Fluids Relat. Interdiscip. Top.*, vol. 74, no. 3, p. 036615, Sep. 2006.
[32] H. Xin, Z. Wu, A. Young, and R. Ziolkowski, "THz thermal radiation enhancement using an electromagnetic crystal," *IEEE Trans. Antennas Propag.*, vol. 56, no. 9, pp. 2970–2980, Sep. 2008.
[33] J. B. Pendry, A. J. Holden, A. J. Robbins, and W. J. Stewart, "Magnetism from conductors and enhanced nonlinear phenomena," *IEEE Trans. Microw. Theory Techn.*, vol. 47, no. 11, pp. 2075–2084, Nov. 1999.
[34] D. R. Smith, W. J. Padilla, D. C. Vier, S. C. Nemat-Nasser, and S. Schultz, "Composite medium with simultaneously negative permeability and permittivity," *Phys. Rev. Lett.*, vol. 84, no. 18, pp. 4184–4187, May 2000.
[35] M. Rahman and M. A. Stuchly, "Transmission line-periodic circuit representation of planar microwave photonic bandgap structures," *Microw. Opt. Technol. Lett.*, vol. 30, no. 1, pp. 15–19, Jul. 2001.
[36] G. V. Eleftheriades, A. K. Iyer, and P. C. Kremer, "Planar negative refractive index media using periodically *L–C* loaded transmission lines," *IEEE Trans. Microw. Theory Techn.*, vol. 50, no. 12, pp. 2702–2712, Dec. 2002.
[37] A. Grbic and G. V. Eleftheriades, "Periodic analysis of a 2-D negative refractive index transmission line structure," *IEEE Trans. Antennas Propag.*, vol. 51, no. 10, pp. 2604–2611, Oct. 2003.
[38] A. Grbic and G. V. Eleftheriades, "An isotropic three-dimensional negative-refractive-index metamaterial," *J. Appl. Phys.*, vol. 98, no. 4, p. 043106, Aug. 2005.
[39] R. R. A. Syms, E. Shamonina, V. Kalinin, and L. Solymar, "A theory of metamaterials based on periodically loaded transmission lines: Interaction between magneto-inductive and electro-magnetic waves," *J. Appl. Phys.*, vol. 97, no. 6, p. 064909, Mar. 2005.
[40] E. Shamonina, "Magnetoinductive polaritons: Hybrid modes of metamaterials with interelement coupling," *Phys. Rev. B, Condens. Matter*, vol. 85, no. 15, p. 155146, Apr. 2012.
[41] R. R. A. Syms and L. Solymar, "Noise in metamaterials," *J. Appl. Phys.*, vol. 109, no. 12, p. 124909, Jun. 2011.
[42] R. R. A. Syms, O. Sydoruk, and L. Solymar, "Lossy metamaterials: No effective medium properties without noise," *Phys. Rev. B, Condens. Matter*, vol. 84, no. 23, p. 235150, Dec. 2011.

Richard R. A. Syms (SM'02) is a Professor of Microsystems Technology with the Electrical and Electronic Engineering Department, Imperial College London, U.K., where he leads the Optical and Semiconductor Devices Group. Prior to that, he was a Reader, Senior Lecturer, and Senior Research Fellow with Imperial College London. Prior to that, he was an Atlas Research Fellow with the Rutherford Appleton Laboratory, Didcot, U.K. He has authored or coauthored over 200 journal and conference papers on volume holography, guided-wave optics, EM theory, microelectromechanical systems, and metamaterials. His current interests are in metamaterials and the development of improved detection systems for magnetic resonance imaging.

R. R. R. Syms is a Fellow of the Royal Academy of Engineering, the Institute of Electrical Engineers (IEE), U.K., and the Institute of Physics.

Oleksiy Sydoruk received the Ph.D. degree in nonlinear applications of magnetoinductive waves from Osnabrück University, Osnabrück, Germany.

He is currently a Junior Research Fellow with the Electrical and Electronic Engineering Department, Imperial College London, London, U.K. Prior to that, he was a Royal Society Newton Research Fellow with Imperial College. Prior to that, he was a Research Fellow at Erlangen University and Osnabrück University. His current research interests are metamaterials and plasmonics, particularly for terahertz source applications.

Laszlo Solymar is currently Senior Research Fellow and Visiting Professor with the Electrical and Electronic Engineering Department, Imperial College London, London, U.K. Prior to that, he was Professor of applied electromagnetism with the Department of Engineering Science, Oxford University, Oxford, U.K. Prior to that, he worked for many years with Standard Telecommunications Laboratories, Harlow, Essex, U.K. He has been published extensively in the fields of communications, EM theory, photorefractive materials, volume holography, superconductivity, traveling-wave electron devices, and antenna arrays. He has also authored many books on similar topics. His most recent interests are RF metamaterials and traveling-wave amplifiers for terahertz frequencies.

Prof. Solymar is a Fellow of the Royal Society and the Institute of Electrical Engineers (IEE), U.K.